Stability Analysis of Discontinuous Galerkin Time-Domain Method for Conductive Media

Mehmet Burak Özakın, Liang Chen, Shehab Ahmed, and Hakan Bagci
Division of Computer, Electrical and Mathematical Science and Engineering
King Abdullah University of Science and Technology (KAUST)
Thuwal 23955-6900, Saudi Arabia
{mehmet.ozakin, liang.chen, shehab.ahmed, hakan.bagci}@kaust.edu.sa

***Abstract*—In this study, the effect of conductivity on the stability of the discontinuous Galerkin time-domain (DGTD) method, which uses Runge-Kutta (RK) or leap-frog (LF) (time-averaging, time-forward, and time-backward) schemes to integrate the Maxwell equations in time, is studied. As a test case, transient reflection from one-dimensional conductive half-space, for which the analytical solution exists, is considered. Numerical results demonstrate that the LF-DGTD schemes, which use time-averaging and time-forward, are significantly more stable and faster than the RK-DGTD scheme for problems involving conductive materials.**

Keywords— Discontinuous Galerkin time-domain method, conductive media, stability analysis.

I. INTRODUCTION

Discontinuous Galerkin time-domain (DGTD) methods have recently gained significant traction within the computational electromagnetics community since they allow for a higher level of flexibility in meshing, have a significantly smaller memory footprint, and are often faster when compared to the classical time-domain finite element schemes [1, 2]. All these benefits stem from the fact that DGTD uses numerical flux to realize information exchange between discretization elements. This yields a block diagonal mass matrix, where the dimension of each block is equal to the number of unknowns in each element. The inverse of this matrix is computed and stored very efficiently before the time integration starts. Consequently, using an explicit time integration scheme yields a very efficient and compact DGTD solver. Indeed, explicit (and high-order) Runge-Kutta (RK) methods are often incorporated within DG frameworks that use high-order nodal polynomial basis functions to discretize the Maxwell equations in space [2].

In this work, we first study the stability DGTD methods that use explicit RK schemes for time integration (termed as RK-DGTD hereinafter) for problems involving conductive materials. Examples of these problems include radiation from metallic antennas, electromagnetic induction, loss prediction on interconnects [3, 4]. Also, note that there is a conductivity term in the formulation of the perfectly matched layers that are used to truncate computation domain [5-8]. To investigate the stability of RK-DGTD, first the time updates are written in a compact form as $\partial_t U(t)|_{t=t_n} = \mathrm{L}(\alpha) U(t_n)$, where the operator $\mathrm{L}(\alpha)$ includes the discretized curl operator, the numerical flux, and the conductivity, parameter α determines the type of the numerical flux, and t_n is the time sample. The eigenvalues of the operator $\mathrm{L}(\alpha)$ are studied for the stability analysis. This study shows that with increasing conductivity, the eigenvalues of $\mathrm{L}(\alpha)$ move out of the stability region, regardless of the type of the numerical flux used. Thus, RK-DGTD becomes unstable for problems involving highly conductive materials unless a very small time-step size is used.

To address this challenge, we propose to switch to a leap-frog (LF) time integration scheme [9, 10]. Inspired from the LF schemes developed for the finite-difference time-domain (FDTD) method [11], we apply time-averaging (TA), time-forward (TF), and time-backward (TB) to the electric field in the conduction current term. To study the stability of the resulting LF-DGTD schemes, we cast the time updates in a compact form as $\bar{U}(t_{n+1}) = G\bar{U}(t_n)$ [12]. For the solution to be stable, all eigenvalues of the matrix G have to be inside the unit circle (stability region). Indeed, unlike the RK-DGTD scheme, for the LF-DGTD schemes with TA and TF, increasing the value of the conductivity does not push these eigenvalues outside the unit circle. As a test case, transient reflection from one-dimensional (1D) conductive half-space, for which the analytical solution exists, is considered. Numerical results demonstrate that the LF-DGTD schemes with TA and TF are always stable as long as the time-step size is chosen based on the Courant-Friedrichs-Lewy (CFL) condition of the same problem without loss.

II. DGTD FOR CONDUCTIVE MEDIA

A. RK-DGTD and LF-DGTD

Discretizing the 1D Maxwell curl equations using nodal basis functions yields:

$$\mu^k \partial_t H_z(t)\big|^k = -D_e E_y(t)\big|^k + \mathrm{M}^{-1} F_H(t)\big|^k, \qquad (1a)$$

$$\varepsilon^k \partial_t E_y(t)\big|^k = -D_h H_z(t)\big|^k + \mathrm{M}^{-1} F_E(t)\big|^k - \sigma^k E_y(t)\big|^k. \qquad (1b)$$

Here, $E_y(t)|^k$ and $H_z(t)|^k$ are the samples of the electric and magnetic fields at the nodes of element k, respectively, ε^k, μ^k, and σ^k are the permittivity, permeability, and conductivity in element k, M is the mass matrix, D_e and D_h are the spatial derivative operators, and $F_H(t)$ and $F_E(t)$ are numerical fluxes [1]. The semi-discretized system (1a)-(1b) is integrated in time by using the explicit fourth-order five-stage low-storage Runge-Kutta scheme [1] to yield the samples of the electric and magnetic fields $E_y|_n^k = E_y(t_n)|^k$ and $H_z|_n^k = H_z(t_n)|^k$ at times $t_n = n\Delta t$, where Δt is the time-step size.

One can also use an LF scheme, which makes use of central difference to approximate the time derivatives, to integrate the system (1a)-(1b). This yields the following time updates on a staggered time grid [10]

$$\mu^k \frac{H_z|_{n+1/2}^k - H_z|_{n-1/2}^k}{\Delta t} = -D_e E_y\big|_n^k + \mathrm{M}^{-1}\left(F_{HE}\big|_n^k + F_{HH}\big|_{n-1/2}^k\right), \qquad (2a)$$

$$\varepsilon^k \frac{E_y\big|_{n+1}^k - E_y\big|_n^k}{\Delta t} = -D_h H_z\big|_{n+1/2}^k + \mathrm{M}^{-1}\left(F_{EH}\big|_{n+1/2}^k + F_{EE}\big|_n^k\right) - \frac{\sigma^k}{2}\left(a E_y\big|_{n+1}^k + b E_y\big|_n^k\right). \quad (2b)$$

In (2b), to implement TA, TF and TB schemes parameter pair (a,b) should be selected as $(1,1)$, $(2,0)$, and $(0,2)$ respectively. On the right hand side, F_{HE}, F_{HH}, F_{EH}, and F_{EE} represent the different numerical flux terms between element k and its neighbors. The system in (2a)-(2b) is used to update the electric and magnetic field samples in an iterative fashion from the known field samples at the previous time step just like it is done with the FDTD method [11].

III. Stability Analysis

In this section, the stability analysis of the RK-DGTD and LF-DGTD schemes for conductive media is explained briefly. The RK-updates used to integrate (1a)-(1b) are written in a compact form as [1]

$$\partial_t U(t)\big|_{t=t_n} = \mathrm{L}(\alpha)U(t_n), \quad (3)$$

where $U=[E_y, H_z]^T$ is the unknown vector, $\mathrm{L}(\alpha)$ is an operator that includes the discretized curl operator, the numerical flux, and the conductivity, and parameter α determines the type of the numerical flux. The stability of the RK-DGTD method is determined by the eigenvalues of $\mathrm{L}(\alpha)$ For the solution to be stable, all eigenvalues of L multiplied by the time-step size have to be inside the RK stability region [2].

In a similar way, the staggered electric and magnetic field time updates in (2a) and (2b) is written in a compact form as [12]:

$$\bar{U}(t_{n+1}) = G\bar{U}(t_n). \quad (4)$$

Here, $\bar{U}(t_n)=[E_y(t_n), H_z(t_{n-1/2})]^T$ is the unknown vector, the matrix $G=[LHS]^{-1}[RHS]$, where

$$[LHS] = \begin{bmatrix} \mathrm{M} + a\left(\frac{\bar{\sigma}^k \Delta t}{2}\right) & \Delta t\bar{D}_h - \Delta t\bar{F}_{EH} \\ 0 & \mathrm{M} \end{bmatrix}, \quad (5)$$

$$[RHS] = \begin{bmatrix} \mathrm{M} + \Delta t\bar{F}_{EE} - b\left(\frac{\bar{\sigma}^k \Delta t}{2}\right) & 0 \\ -\Delta t\bar{D}_e + \Delta t\bar{F}_{HE} & \mathrm{M} + \Delta t\bar{F}_{HH} \end{bmatrix}, \quad (6)$$

$$\bar{\sigma}^k = \frac{\mathrm{M}\,\sigma^k}{\varepsilon^k}, \quad (7)$$

$$\bar{D}_e = \frac{\mathrm{M}\,D_e}{\mu^k}, \quad \bar{D}_h = \frac{\mathrm{M}\,D_h}{\varepsilon^k}, \quad (8)$$

$$\bar{F}_{HE} = \frac{F_{HE}}{\mu^k}, \bar{F}_{HH} = \frac{F_{HH}}{\mu^k}, \bar{F}_{EH} = \frac{F_{EH}}{\varepsilon^k}, \bar{F}_{EE} = \frac{F_{EE}}{\varepsilon^k}. \quad (9)$$

For the time updates (2a)-(2b) to be stable, all eigenvalues of G have to be inside the unit circle.

TABLE I. MAXIMUM CFLN AND CORRESPONDING TIME-STEP SIZES AND SIMULATION TIMES FOR RK-DGTD AND LF-DGTD

		CFLN	Δt [s]	Simulation Time [m]
RK-DGTD		0.0073	4.03×10^{-17}	3960
LF-DGTD	*TA*	0.28	1.55×10^{-15}	5.7
	TF	0.28	1.55×10^{-15}	5.3
	TB	0.0031	1.71×10^{-17}	318.2

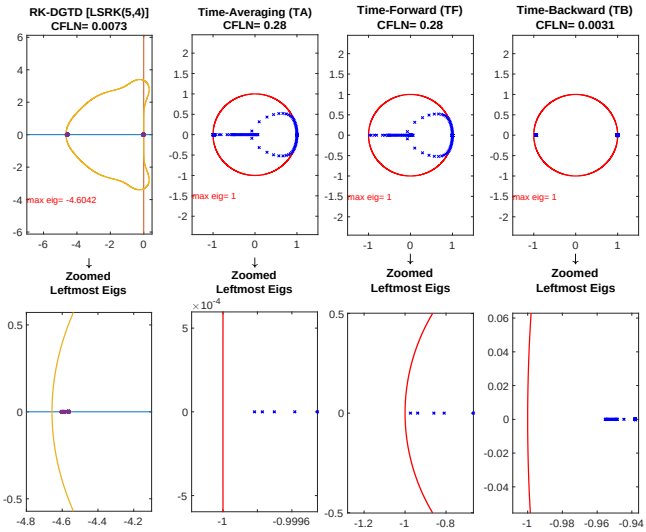

Fig. 1. Eigenvalues of RK-DGTD and LF-DGTD schemes and the stability regions.

IV. Numerical Results

In this section, as a test case, transient reflection from 1D conductive half-space is studied. The problem space consists of two half spaces: free space (of length 42μm) and highly electrically conductive material (of length 138μm) with conductivity 10^6 S/m. A monochromatic plane wave with frequency 1GHz is located in the free space and waves propagate only towards the conductive medium. The excitation is applied for a duration of ten periods. Note that the skin depth of the conductive medium at 1GHz is 15.9μm. To resolve the skin depth accurately, the discretization element length is selected as 1.66μm, which yields a total of 30 elements in the whole computation domain. The order of basis functions is three. The first order absorbing boundary condition (which is exact in 1D) is used at outer boundaries of the computation domain.

Several simulations are carried out to find the maximum CFL number (CFLN) of RK-DGTD and LF-DGTD with TA, TF, and TB. These values are presented in Table I. Table I also present the corresponding values of Δt and the computation times. The eigenvalues of L and G are computed using these values of Δt (Fig. 1). These results show that LF-DGTD with TA and TF use the largest time step size and consequently has the shortest simulation time.

To demonstrate the accuracy of the DGTD schemes, numerical results are compared with results obtained using closed form expressions [13]. First, we select an observation point in the conductive half space (90μm away from interface). Electric field computed using the DGTD schemes at this point match very well with the analytical solution as shown in Fig. 2.

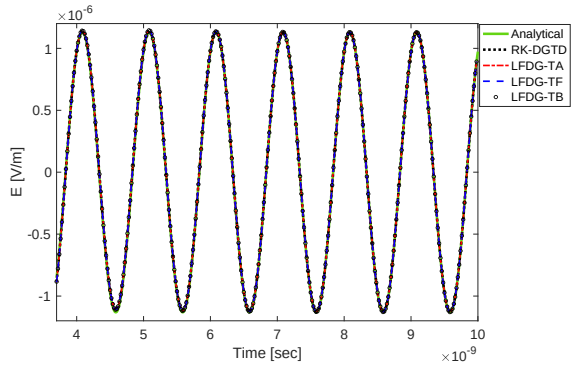

Fig. 2. Time-domain electric field at the observation point inside the conductive half-space.

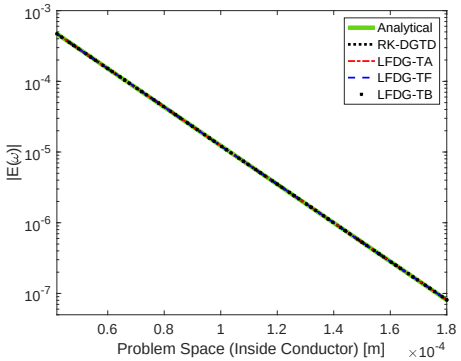

Fig. 3. Decay of the electric field inside the conductive half-space.

Next, the decay of the electric field in the conductive half-space is demonstrated. Frequency-domain electric field amplitude is extracted from the time-domain DGTD simulations and compared to that obtained using the closed form expression [13]. Results presented in Fig. 3 show the accuracy of all four DGTD schemes.

V. Conclusion

In this study, the effect of conductivity on the stability of RK-DGTD and LF-DGTD is investigated. As a test case, transient reflection from 1D conductive half-space is considered. Numerical results demonstrate that the LF-DGTD with TA and TF use significantly larger time steps than the RK-DGTD scheme, and therefore is faster, for problems involving conductive materials.

References

[1] J. S. Hesthaven and T. Warburton, Nodal Discontinuous Galerkin Methods: Algorithms, Analysis, and Applications, Springer Science & Business Media, 2008.

[2] K. Busch, M. Koenig, and J. Niegemann, “Discontinuous Galerkin methods in nanophotonics”, Laser & Photonics Reviews, vol. 5, no. 6, pp. 773-809, 2011.

[3] J. Yang, W. Cai, and X. Wu, “A high-order time domain discontinuous Galerkin method with orthogonal tetrahedral basis for electromagnetic simulations in 3-D heterogeneous conductive media,” Communications in Comp. Phys., vol. 21, no. 4, pp. 1065-1089, 2017.

[4] M. B. Ozakin, L. Chen, S. Ahmed, and H. Bagci, “Computation of fields from a magnetic dipole in a conductive medium using the QS-DGTD method,” in *International Applied Computational Electromagnetics Society Symposium (ACES)*, Miami, Florida, USA, Apr. 14-18, 2019.

[5] T. Lu, P. Zhang, and W. Cai, “Discontinuous galerkin methods for dispersive and lossy Maxwell's equations and PML boundary conditions,” J. of Comp. Phys., vol. 200, no. 2, pp. 549-580, 2000.

[6] J. Li, “Development of discontinuous galerkin methods for Maxwell’s equations in metamaterials and perfectly matched layers,” J. of Comp. and App. Math., vol. 236, no. 5, pp. 950-961, 2011.

[7] L. Chen, M. B. Ozakin, S. Ahmed, and H. Bagci, “A memory-efficient implementation of perfectly matched layer with smoothly-varying coefficients in discontinuous galerkin time-domain method,” IEEE Trans. Antenna Propag. 1-1, doi: 10.1109/TAP.2020.3037651.

[8] L. Chen, M. B. Ozakin, and H. Bagci, “A low-storage PML implementation within a high-order discontinuous Galerkin time-domain method,” in *Proc. IEEE Int. Symp. Antennas Propag.*, Montréal, Québec, Canada, Jul. 5-10, 2020, pp. 1069–1070.

[9] J. Alvarez, L. Angulo, A. R. Bretones, and S. G. Garcia, “A spurious-free discontinuous galerkin time-domain method for the accurate modeling of microwave filters,” IEEE Trans. Microw. Theory Techn., vol. 60, no. 8, pp. 2359-2369, 2012.

[10] J. Alvarez, L. D. Angulo, A. R. Bretones, M. R. Cabello, and S. G. Garcia, “A leap-frog discontinuous Galerkin time-domain method for HIRF assessment,” IEEE Trans. on Electromagnetic Comp., vol. 55, no. 6, pp. 1250-1259, 2013.

[11] A. Taflove and S. C. Hagness, Computational Electrodynamics: The Finite-Difference Time-Domain Method, Artech House, 2005.

[12] R. F. Remis, “On the stability of the finite-difference time-domain method”, J. of Comp. Phys., vol. 163, no. 1, pp. 249-261, 2000.

[13] C. A. Balanis, Advanced Engineering Electromagnetics, 2nd ed., John Wiley & Sons Inc., 2012.